

Multi-bubble motion behavior of electric field based on phase field model

Chang-Sheng Zhu(朱昶胜), Dan Han(韩丹), Li Feng(冯力), Sheng Xu(徐升)

Citation: Chin. Phys. B . 2019, 28(3): 034701. **doi:** 10.1088/1674-1056/28/3/034701
Journal homepage: http://cpb.iphy.ac.cn; http://iopscience.iop.org/cpb

What follows is a list of articles you may be interested in

Molecular-dynamics investigation of the simple droplet critical wetting behavior at a stripe pillar edge defect

Xiaolong Liu(刘小龙), Chengyun Hong(洪成允), Yong Ding(丁勇), Xuepeng Liu(刘雪朋), Jianxi Yao(姚建曦), Songyuan Dai(戴松元)

Chin. Phys. B . 2019, 28(1): 014703. **doi:** 10.1088/1674-1056/28/1/014703

Derivation of lattice Boltzmann equation via analytical characteristic integral

Huanfeng Ye(叶欢锋), Bo Kuang(匡波), Yanhua Yang(杨燕华)

Chin. Phys. B . 2019, 28(1): 014701. **doi:** 10.1088/1674-1056/28/1/014701

Phase field simulation of single bubble behavior under an electric field

Chang-Sheng Zhu(朱昶胜), Dan Han(韩丹), Sheng Xu(徐升)

Chin. Phys. B . 2018, 27(9): 094704. **doi:** 10.1088/1674-1056/27/9/094704

Physical and chemical effects of phosphorus-containing compounds on laminar premixed flame

Yongfeng Yin(殷永丰), Yong Jiang(蒋勇), Rong Qiu(邱榕), Caiyi Xiong(熊才溢)

Chin. Phys. B . 2018, 27(9): 094701. **doi:** 10.1088/1674-1056/27/9/094701

A multicomponent multiphase lattice Boltzmann model with large liquid-gas density ratios for simulations of wetting phenomena

Qing-Yu Zhang(张庆宇), Dong-Ke Sun(孙东科), Ming-Fang Zhu(朱鸣芳)

Chin. Phys. B . 2017, 26(8): 084701. **doi:** 10.1088/1674-1056/26/8/084701

Multi-bubble motion behavior of electric field based on phase field model*

Chang-Sheng Zhu(朱昶胜)[1,2,†], Dan Han(韩丹)[1], Li Feng(冯力)[2], and Sheng Xu(徐升)[1]

[1] School of Computer and Communication, Lanzhou University of Technology, Lanzhou 730050, China
[2] State Key Laboratory of Gansu Advanced Processing and Recycling of Non-Ferrous Metal, Lanzhou 730050, China

(Received 11 October 2018; revised manuscript received 6 December 2018; published online 25 February 2019)

By coupling the phase field model with the continuity equation of incompressible fluid, Navier–Stokes equation, electric field equation, and other governing equations, a multi-field coupling model for multi-bubble coalescence in a viscous fluids is established. The phase field method is used to capture the two-phase interface. The motion and coalescence of a pair of coaxial bubbles under an external uniform electric field and the effects of different electric field strengths on the interaction and coalescence of rising bubbles are studied. The results show that the uniform electric field accelerates the collision and coalescence process of double bubbles in the fluid, and increases the rising velocity of the coalesced bubble. The electric field with an intensity of $E = 2$ kV/mm is reduced about 2 times compared with that without electric field in coalescence time. When the electric field strength is strong ($E \geq 1$ kV/mm), the coalesced bubble will rupture before it rises to the top of the calculation area, and the time of the bubble rupturing also decreases with the increase of the electric field strength. The phase field method is compared with the simulation results of Lattice Boltzmann Method (LBM), and the shape of bubble obtained by the two methods is in good agreement, which verifies the correctness of the calculation model.

Keywords: electro-hydro dynamics, multi-bubble, phase field

PACS: 47.11.–j, 47.55.dd **DOI:** 10.1088/1674-1056/28/3/034701

1. Introduction

The hydrodynamics of water vapor multi-phase motion has been widely found in nature and engineering practice. The collision and coalescence of a pair of bubbles occurs frequently in two-phase bubble flows. The movement and interaction of the bubbles in the liquid can significantly affect the contact time and area of gas–liquid, and change the heat and mass transfer and chemical reaction of the gas–liquid system. Therefore, a large number of experiments and numerical simulations on the motion and interaction of bubbles in liquids have been carried out.[1–3]

Zhang *et al.*[4] simulated and analyzed the interaction between bubbles from two angles of side-by-side arrangement and up-and-down arrangement, with an emphasis on the influence of fluid viscosity and bubble spacing on the interaction. Annaland *et al.*[5] used a 3D gas–liquid model characterized by a large density and viscosity ratio and a large value of the surface tension coefficient to simulate co-axial and oblique coalescence of two rising gas bubbles. Cheng *et al.*[6] gave a three-dimensional numerical simulation of multiple bubbles rising under buoyancy in a quiescent viscous incompressible fluid, and presented the numerical results about the evolution of bubble shapes, instantaneous streamlines and velocity distribution for the co-axial and oblique coalescence of two bubbles rising in a viscous fluid, and the behavior of bubbly flow in a square duct. Li *et al.*[7] used Fluent software to numerically simulate the interaction between in-line two bubble in non-Newtonian fluids. The results showed the interaction between leading bubble and following bubble was related to center distance between the two bubbles. Lv *et al.*[8] studied the merging of two bubbles in two dimensions as well as in three dimensions, obtained the critical conditions of bubble coalescence, and used the three dimensions model to study the bubble deformation in shear flow. Hadidi and Jalali-Vahid[9] numerically simulated the coaxial coalescence of a pair of bubbles rising in a viscous liquid column under different external uniform magnetic fields. The results showed that the uniform magnetic field accelerates the coalescence of bubble pairs in the dielectric fluid and enhances the rising velocity of the bubble.

The motion deformation and topological structure of the gas–liquid interface is one of the main problems in numerical simulation. So in order to deal with the multi-phase flow interface correctly, researchers have proposed many methods.

Volume of fluid (VOF) method can automatically deal with nonlinear phenomena, but it is difficult to calculate the curvature of the interface because it cannot give accurate information about the position and shape of the interface. Therefore, it is difficult to deal with the problem of multi-phase motion which needs to consider the surface tension.[10,11] level-

*Project supported by the National Natural Science Foundation of China (Grant Nos. 51661020, 11504149, and 11364024), the Postdoctoral Science Foundation of China (Grant No. 2014M560371) and the Funds for Distinguished Young Scientists of Lanzhou University of Technology, China (Grant No. J201304).

†Corresponding author. E-mail: zhucs2008@163.com;zhucs@lut.edu.cn

© 2019 Chinese Physical Society and IOP Publishing Ltd

set method only needs to calculate the function value near the interface, which greatly reduces the calculation time. However, it can not lead to the conservative property[12,13] because of the initialization of the function artificially. Phase-field method, introduces a phase variable into the flow field to control the motion of the interface by updating the Cahn–Hilliard (C–H) equation of the phase variable. It can deal with multi-phase of the complex set topology change of the interface, including complex structural changes such as splitting and coalescence of interfaces.[14,15]

LBM method has the characteristics of easy boundary setting and is good at dealing with complex and irregular structures. It is widely used in the simulation and research of many kinds of flow problems.[16,17] The interface information functions in the VOF and Level-set methods are the volumetric ratio of the fluid, independent of the flow parameters and the distance symbol function of the interface respectively. The phase variable in the phase field method is physical quantities associated with the flow parameters. On this basis, the C–H equation is coupled with the flow governing equation to avoid the destruction of the physical conservation caused by manual processing near the interface, which becomes a powerful method for numerical simulation of multi-phase flow.

The interaction between bubbles is an important phenomenon in two-phase flow. Applying an electric field to control bubble dynamics is an attractive and unavoidable method. Therefore, in this study, a two-dimensional (2D) phase field model in which the electric field and the flow field cooperate is established. The motion and coalescence law of the double bubble are discussed, and the interface position of the two-phase fluid is accurately captured. The effects of uniform electric field on the interaction and coalescence of multiple bubbles in fluid phase and the relationship between different electric field strengths and bubble coalescence rates were investigated.

2. Mathematical model

In this study, the governing equations of two-phase flow under the effects of an external uniform electric field consists of the conservation equations of continuity and momentum, phase field equations and the electric field equation, which is obtained by simplification of Maxwell's equations.

2.1. Flow field equation

Assuming that the two-phase Newtonian fluids are incompressible and incompatible, the diffusion effect at the interface is equivalent, and the convective velocity satisfies the divergence of zero, then the continuity equation reads

$$\nabla \cdot \boldsymbol{u} = 0. \tag{1}$$

The whole flow field governing equation is described by a 2D incompressible Navier–Stokes equation[5,15]

$$\rho(\phi)\left(\frac{\partial \boldsymbol{u}}{\partial t} + (\boldsymbol{u}\cdot\nabla)\boldsymbol{u}\right) = -\nabla p + \nabla\cdot\left[\mu(\phi)\left(\nabla\boldsymbol{u} + \nabla\boldsymbol{u}^{\mathrm{T}}\right)\right] + \rho(\phi)g + F_{\mathrm{st}} + F_{\mathrm{e}}, \tag{2}$$

where $\boldsymbol{u}$ is the velocity vector of the fluid, $\rho(\phi)$ is the local averaged density, t is the time, p is the pressure, $\mu(\phi)$ is the dynamic viscosity coefficient, $\rho(\phi)g$ is gravity, F_{st} is the source of surface tension, g is gravitational acceleration, and F_{e} is the external force, which is referred to herein as the electric field force.

2.2. Phase field model

The phase field method has a unique advantage in solving the two-phase flow motion with large deformation in the region. Cahn–Hilliard equation[18–20] is used to track the diffusion interface of gas–liquid two-phase flow. The calculation equation is decomposed into two partial differential equations as follows:

$$\frac{\partial \phi}{\partial t} + \nabla\cdot(\phi\boldsymbol{u}) = \nabla\cdot\gamma\nabla G, \tag{3}$$

$$\varphi = -\nabla\cdot\xi^2\nabla\phi + \left(\phi^2 - 1\right)\phi. \tag{4}$$

Phase field method obtains the position information of the interface through the phase field variable. The change of the dimensionless phase field parameter ϕ from -1 to 1 reflects the change of the interface. It is equal to 1 for gas and 0 for fluid around the bubble. G is the chemical potential, and its expression is

$$G = \lambda\left[-\nabla^2\phi + \frac{\left(\phi^2-1\right)\phi}{\xi^2}\right] = \frac{\lambda}{\xi^2}\varphi, \tag{5}$$

where φ is the auxiliary variable of the phase field, γ is the mobility parameter, whose value determines the time factor of the Cahn–Hilliard equation diffusion with a given value of 1. ξ is the parameter that determines the thickness of the diffusion interface. $\xi \to 0$: when the mixed energy density λ and the surface tension coefficient σ[20] satisfy the following relationship:

$$\lambda = \frac{3\sigma\xi}{\sqrt{8}}. \tag{6}$$

2.3. Electric field equation

The potential of any point in the region can be solved according to the Laplace equation[21] with variable permittivity

$$-\nabla\cdot(\varepsilon_0\varepsilon(\phi)\nabla V) = 0, \tag{7}$$

where ε_0 is the dielectric constant of vacuum, 8.8542×10^{-12} F/m, $\varepsilon(\phi)$ for the fluid relative permittivity, potential V can be expressed by electric field strength E[21]

$$E = -\nabla V. \tag{8}$$

The Maxwell stress tensor T due to the difference in electrical properties at the interface of the two phases can be expressed as[21,22]

$$T = \varepsilon_0 \varepsilon(\phi) \left[EE - \frac{1}{2}(E \cdot E) I \right], \tag{9}$$

where I is the second-order unit tensor. In the solution domain, the Maxwell stress tensor is 0 except for the other positions in the two-phase interface.

The bubble under the action of the electrostatic field F_e can be given by the divergence of the Maxwell stress tensor T

$$F_e = \nabla \cdot T. \tag{10}$$

Therefore, the electric field force F_e can be expressed as

$$F_e = \nabla(\varepsilon_0 \varepsilon(\phi) EE) - \frac{1}{2} E^2 \nabla \varepsilon_0 \varepsilon(\phi). \tag{11}$$

2.4. Surface tension

The surface tension is equivalent to the product of the gradient of the field variable and the chemical potential, which is added to the N–S equation (2) as a volume force to solve the two-phase flow:

$$F_{st} = G \nabla \phi. \tag{12}$$

2.5. Fluid properties parameters

In the numerical simulation study of the two-phase flow field, there are corresponding flow parameters that can characterize the characteristics of the two-phase fluid, which vary with time and position. On the premise that the phase variable ϕ is given in the full flow field, the local average density $\rho(\phi)$, viscosity coefficient $\mu(\phi)$, and relative permittivity $\varepsilon(\phi)$ of the flow field are obtained by the following formula:

$$\rho(\phi) = \frac{1+\phi}{2}\rho_g + \frac{1-\phi}{2}\rho_l, \tag{13}$$

$$\mu(\phi) = \frac{1+\phi}{2}\mu_g + \frac{1-\phi}{2}\mu_l, \tag{14}$$

$$\varepsilon(\phi) = \frac{1+\phi}{2}\varepsilon_g + \frac{1-\phi}{2}\varepsilon_l, \tag{15}$$

where the subscript "g" represents the gas phase, and the subscript "l" represents the liquid. It can be seen from the above formula, that the local density and viscosity in the flow field and the relative dielectric constant are composed of two parts, which are derived from two kinds of phase.

3. Initial conditions

3.1. Geometric motion model

We aim to simulate the motion, interaction, and coalescence of a pair of gas bubbles in a viscous liquid under the effects of a uniform electric field (vertical electric field E). The motion area of bubbles is shown in Fig. 1.

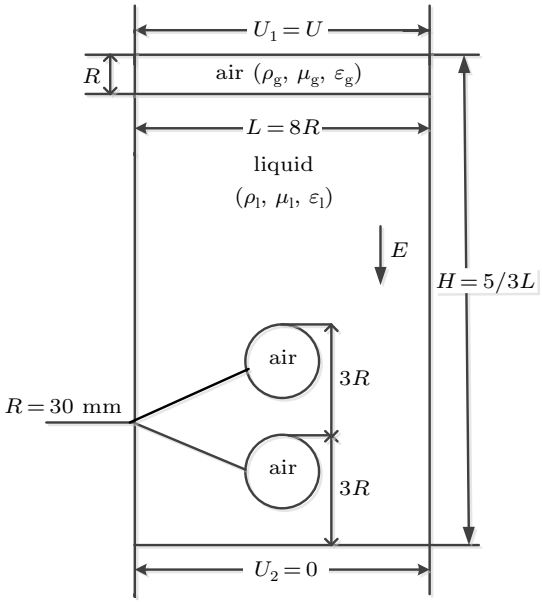


Fig. 1. Schematic diagram of 2D geometrical model in numerical simulation.

According to the existing research results, the terminal rising velocity of the bubble is not affected by the size of the calculation domain, and the size of the calculation area is expected to exceed 3 to 4 times the initial bubble diameter.[5] In the 2D plane gas–liquid simulation model shown in Fig. 1, the solution domain is $L \times H$, a double bubble having a radius of R, a viscosity of μ_g, and a dielectric constant of ε_g is in a liquid with a viscosity of μ_l and a dielectric constant of ε_l. The initial shape of the double bubble is spherical and incompatible with the external liquid, the vertical distance between the two bubbles is R, and the initial velocity of the bubbles is 0 m/s.

3.2. Boundary condition

The fluid considered in this paper is a viscous fluid with good wettability and adherence to the wall. If there is no slip on the wall, then the wall function is

$$u = 0. \tag{16}$$

3.3. Initial condition setting

The flow field of the bubble is studied as a low Reynolds number flow field with a density ratio of two phases of 1000 and a viscosity ratio of 100. The main physical parameters used in the simulation are shown in Table 1.[15]

Table 1. Material properties in the model.

	Liquid	Air
ρ/kg·m^{-3}	1000	1
μ/Pa·s	1.16	0.0116
ε	81.5	1
σ/N·m^{-1}	0.0728	–

4. Results and analysis

4.1. Result verification

The following two dimensionless parameters are used to describe the motion characteristics of the bubble: E_o for the Eotvos number, M_o for the Morton number.

$$E_o = \frac{g\left(\rho_l - \rho_g\right) d^2}{\sigma}, \tag{17}$$

$$M_o = \frac{g(\rho_l - \rho_g)\mu_l^4}{\rho_l^2 \sigma^3}, \tag{18}$$

where d is the bubble diameter, M_o represents the property of the external fluid, and E_o characterizes the ratio of the float lift to the surface tension. These two parameters are controllable. The Morton number and Eotvos number used in this model are 46 and 484, respectively.

By coupling the governing equations (1)–(15) and using Comsol software, we studied the interaction and coalescence of two identical spherical bubbles centered on a vertical line in a viscous liquid. Before the numerical simulation of the problem, firstly the test of mesh independency has been carried out and results are shown in Fig. 2. It can be concluded that when the mesh size is equal to 2 mm, the position and coalescence time of the two bubbles are independent of the mesh size. Therefore, this mesh size was used as a correct mesh size to solve the coupled governing equations.

The phase field method is used to solve the two-phase flow governing equation of the coupled electric field. The

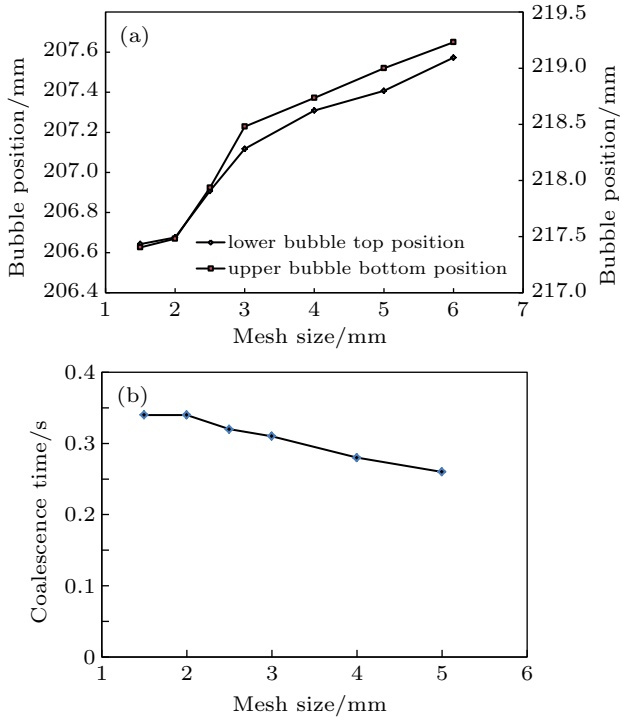


Fig. 2. Mesh independency test. (a) The effect of different mesh sizes on the position of double bubbles; (b) Influence of different mesh size on the coalescence time of double bubbles.

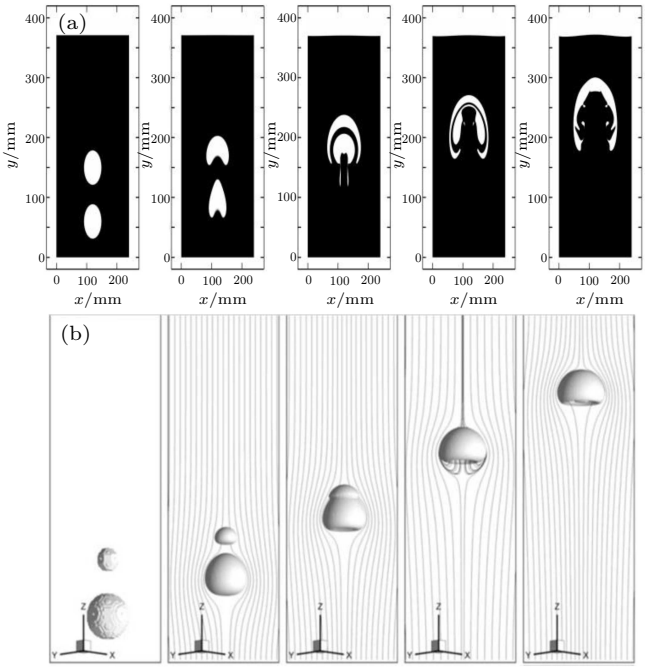


Fig. 3. Comparison of the coalescence of in-line vertical bubbles obtained in this research with numerical; (a) results of present research using the phase field method; (b) numerical results of Cheng *et al.*[6] obtained using the LBM method with $M_o = 41.1$.

motion behavior of the coaxial double rising bubbles placed vertically in the stationary liquid is studied. The simulation results are shown in Fig. 3(a). In order to verify the reliability of the simulation, the simulation results are compared with the numerical results obtained by Cheng *et al.*[6] using LBM method. As shown in Fig. 3(b), there is a good qualitative agreement between the two results.

4.2. Influence of electric field intensity on vertical double bubble coalescence behavior

In order to study the influence of electric field strength on the vertical double-bubbles coalescence behavior, the simulation was carried out on two cases: low electric field strength ($E \leq 0.75$ kV/mm) and high electric field strength ($E \geq 1$ kV/mm). Figure 4 shows the influen- ce of the uniform electric field on the dynamics and deformation of the bubbles when the electric field strength is low.

The first behavior shown in Fig. 4 is the dynamic behavior of a pair of bubbles placed up and down without an electric field ($E = 0.0$ kV/mm). Due to the wake effect of the upper bubble, a low pressure zone is formed behind it, which causes a suction effect on the lower bubble, and causes the lower bubble to rise faster than the upper bubble. This is because the resistance acting on the lower bubble is less than that of the upper bubble.

When the rising velocity of the lower bubble is greater than the velocity of the upper bubble, the distance between the both bubble gets closer and closer, so that collision and coalescence of the bubble eventually occur. As shown in Fig. 4,

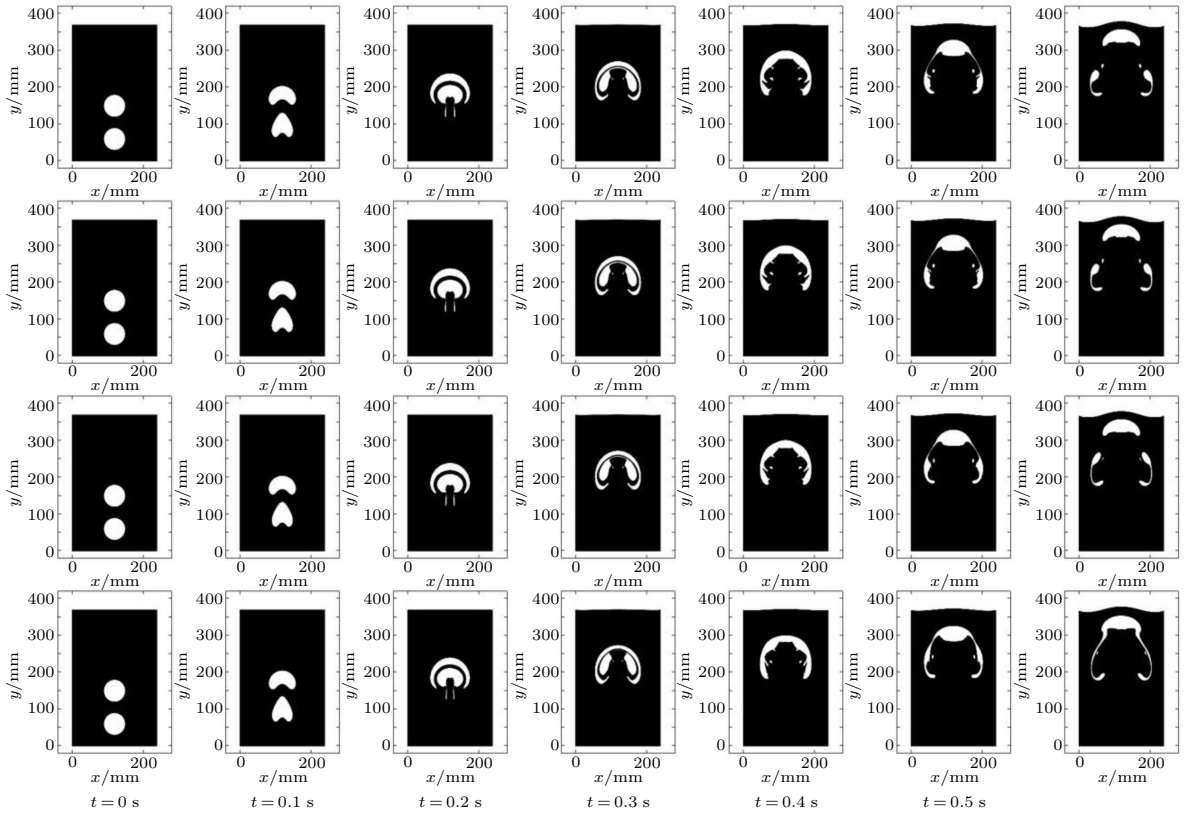


Fig. 4. Effect of low-intensity electric field on the interaction of double bubbles at different times. First line: $E = 0$ kV/mm; second line: $E = 0.25$ kV/mm; third line: $E = 0.5$ kV/mm; fourth line: $E = 0.75$ kV/mm.

the distance between the lower bubble and the upper bubble is significantly reduced during the rise from $t = 0$ to 0.3 s, and finally the two bubbles coalescence at $t = 0.34$ s. After the coalescence of the two bubbles, as the coalescence range increases, the coalescence becomes a large sphere and begins to rise. Similar to the rise of a single bubble, the bubble gradually rises and a significant concave motion appears at the bottom of the bubble. Over time, the indentation at the bottom of the bubble became more and more serious, causing two arc-shaped bulges ($t = 0.4$ s) to be formed on the left and right sides. The motion velocity of the interface below the bubble is greater than that of the upper one. The shape of the bubble is continuously developed, forming a crescent shape as a whole. The two gas snares formed on the left and right sides of the bubble are separated from the main bubble and becomes two separate small bubbles, while the rest of the bubble will continue to move upward at a certain speed. Move ($t = 0.6$ s), it should be noted that if the initial distance between the bubbles will be higher so that the wake of the leading bubble could not affect the trailing bubble sufficiently, then there is no merging between them.

At the same time, figure 4 also shows the simulation results of the influence of the applied electric field on the bubble behavior of 0.25 kV/mm, 0.5 kV/mm, and 0.75 kV/mm, respectively. It can be seen that the applied electric field has a certain influence on the dynamics of the bubbles. When $t = 0.3$ s and the electric field strength E is 0.75 kV/mm, the distance between the bubbles is smaller than that strength of 0 kV/mm, 0.25 kV/mm and 0.5 kV/mm. With the decrease of the distance between the bubbles, the coalescence process of bubbles will occur earlier. Similarly, the applied electric field also affects the final shape of the combined bubble. As the electric field strength increases, the indentation at the bottom of the bubble becomes more severe, as shown in $t = 0.6$ s.

The effect of the electric field intensity ($E \geq 1$ kV/mm) on the coalescence of double bubbles is shown in Fig. 5. In this figure, the effects of applied electric fields of 1 kV/mm, 1.25 kV/mm, 1.25 kV/mm, 1.5 kV/mm, and 2 kV/mm are given, and the results are compared with those of bubble rising without electric field effect at different times. The results show that the applied electric field has a certain influence on the vertical elongation of the bubbles. As the bubbles elongate in the vertical direction, their distance decreases faster, allowing the bubbles to coalescence together faster. The variation of the distance between the double bubble over time by the applied electric field of different intensities is shown in Fig. 6. By comparing the effects of electric fields of different intensities, the results show that the distance between bubbles decreases with the increase of electric field intensity (at the same time), which leads to faster collision and coalescence of the double bubble. Therefore, the coalescence of the bubbles occurs around $t = 0.1$ s when $E = 2$ kV/mm, and about $t = 0.34$ s when there is no electric field.

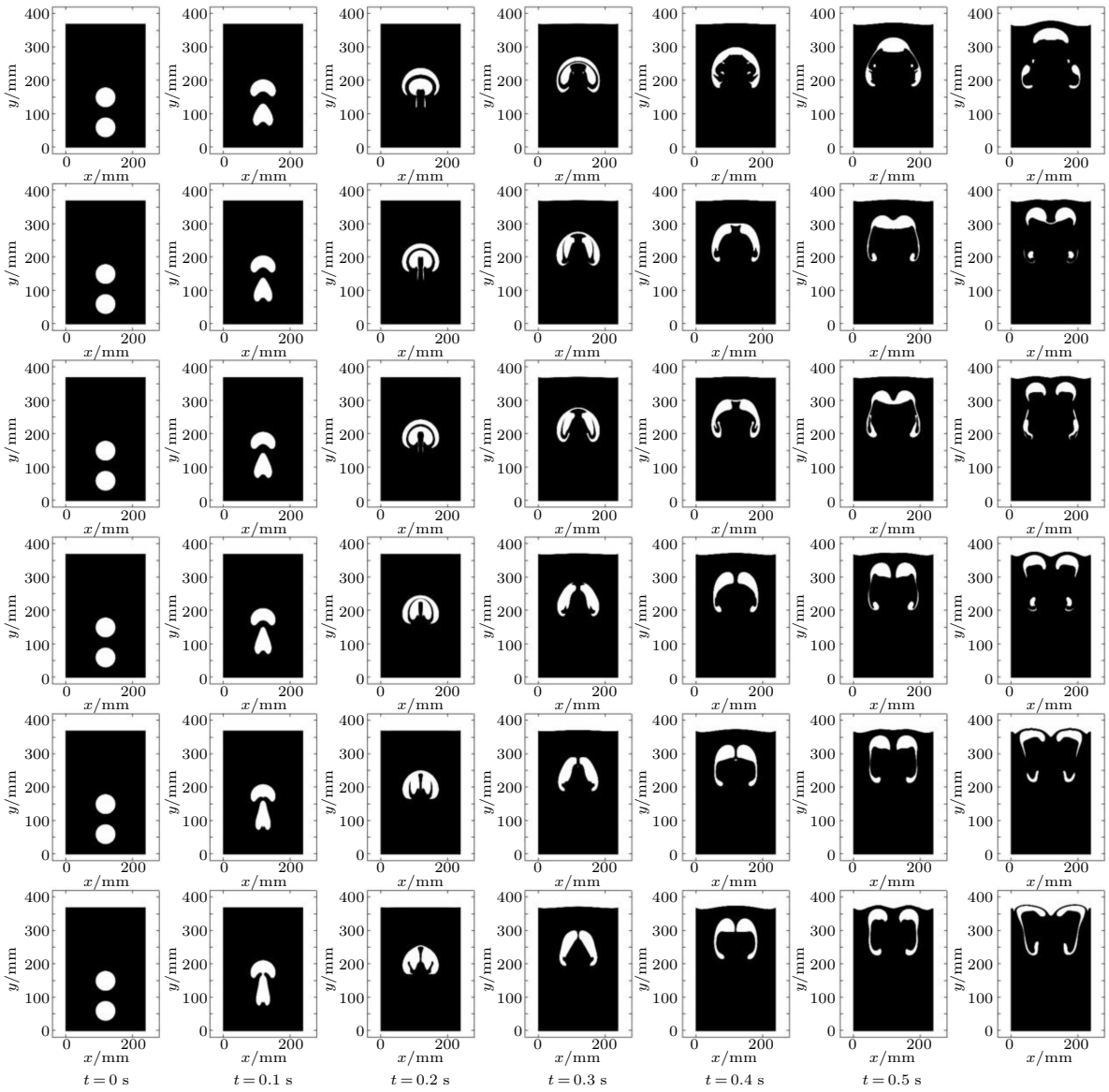


Fig. 5. Effect of high-intensity electric field on the interaction of double bubbles at different times. First line: $E = 0$ kV/mm; second line: $E = 1$ kV/mm; third line: $E = 1.25$ kV/mm; fourth line: $E = 1.5$ kV/mm; fifth line: $E = 1.75$ kV/mm; sixth line: $E = 2.0$ kV/mm.

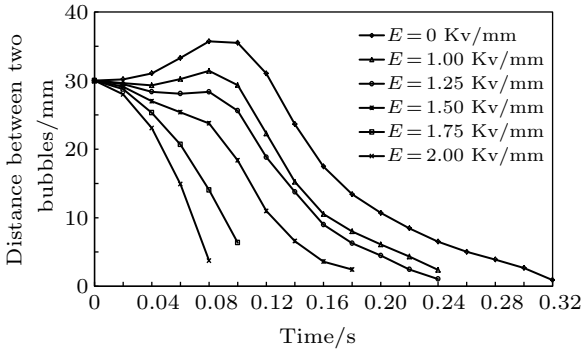


Fig. 6. Effect of different electric field intensity on the distance between two bubbles.

The effect of the different intensity of the applied electric fields on the coalescence time of the double bubble placed top and bottom is shown in Fig. 7. Obviously, the uniform electric field is applied to reduce the time of bubble collision and coalescence. The low electric field intensity (up to 0.75 kV/mm) has little effect on the bubble coalescence time, while the strong electric field has a great influence on the bubble coalescence time. As can be seen from Fig. 7, the electric field having an intensity of $E = 2$ kV/mm is reduced by about 2 times the coalescence time as compared with the case without the electric field. The interaction between bubbles is an important phenomenon in two-phase flow. The application of an external uniform electric field capable of controlling bubble interaction can play an important role in the control of two-phase flow from the point of view of hydrodynamics and heat transfer characteristics. In addition, it has been found that intensity increases to a certain extent, the surface tension of the fused bubble is not enough to maintain the shape of the bubble, and the electric field force will penetrate the bubble from the center, and the bubble will be broken. Figure 8 shows the bursting

time of bubbles under different electric field strengths. It can be seen from the figure that the bursting time of the bubble is inversely proportional to the applied electric field strength, and the stronger electric field force will penetrate the bubble earlier.

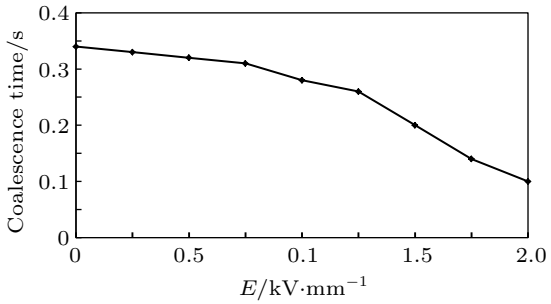


Fig. 7. Influence of different electric field intensity on the coalescence time of double bubbles.

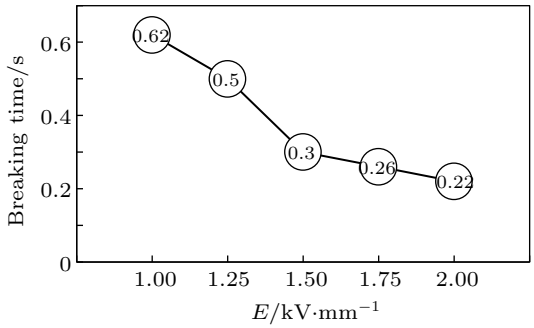


Fig. 8. Effect of different electric field intensity on bubble breaking time after coalescence.

Figure 9 shows the instantaneous streamlines, the velocity vector distribution and bubbles shape evolution with time in the corresponding flow field ($E = 1$ kV/mm) at time $t = 0.1$ s and $t = 0.2$ s. The streamlines around the bubbles not only show symmetrical distribution along the vertical axis of the bubbles, but also show symmetrical distribution at the head and rear of the sphere. It can be clearly seen from the figure that a recirculation zone is formed on the left and right sides of the double bubbles. It is formed by a pair of symmetrical vortices, which causes the liquid in front of the bubbles to flow into the wake of the bubbles. The continuous motion of the eddy eventually causes small bubbles to appear below and separate from the main bubbles. Compared with the rising and changing shape of a single bubble in the liquid, the guided bubbles rise as isolated bubbles. As time goes, the dominant bubble develops into a flat ellipse, and the tail becomes significantly elongated in the vertical direction due to the interaction between the bubble, and the bubble becomes conical and elongated in shape.

Figure 10 shows the distribution of the electric field and polarization intensity in the solution domains with strength of 0.25 kV/mm and 1.25 kV/mm at different times. Red is the electric field line and the legend color is the polarization intensity. It can be seen that the electric field force acts only

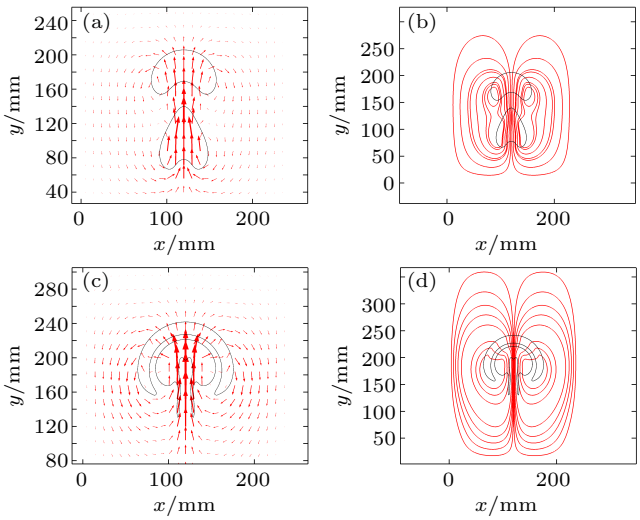


Fig. 9. Velocity vector field and instantaneous streamline diagram in flow field. (a), (b) $t = 0.1$ s, (c), (d) $t = 0.2$ s.

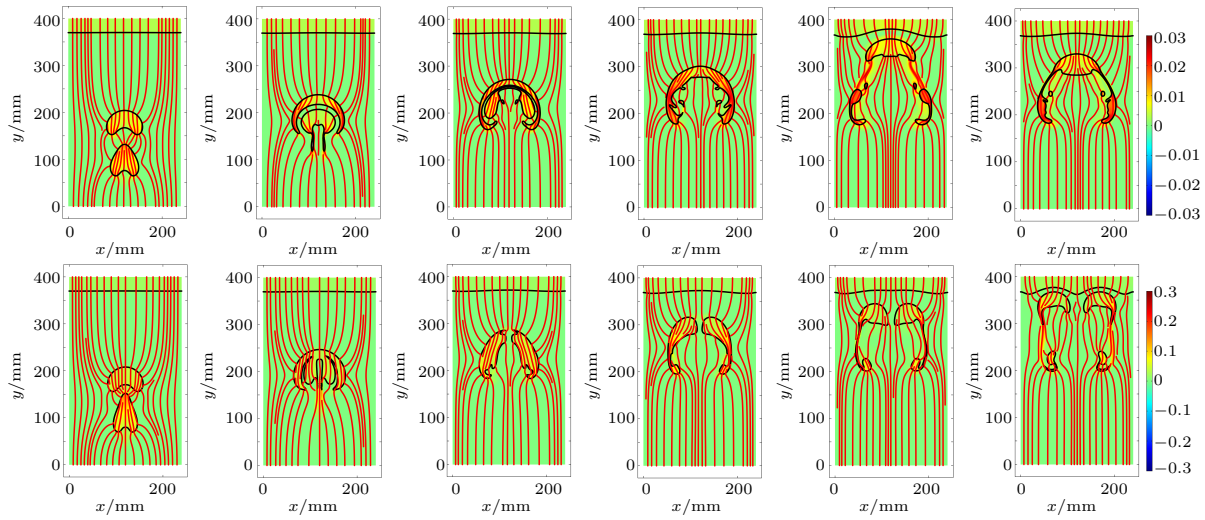


Fig. 10. Distribution of electric field lines and polarization. Top panels: $E = 0.25$ kV/mm, bottom panels: $E = 1.5$ kV/mm.

on the interface of the gas-liquid two-phase flow, and the bubbles are significantly deformed under the action of the electric field. The electric field force acting on the bubbles tends to compress the bubble in the horizontal direction which results in elongation of the bubbles in the direction of applied electric field (vertical direction) and consequently reduction the cross-sectional area of the bubbles.

5. Conclusions

In this paper, phase-field method was used to simulate the gas-liquid two-phase flow. The coupling effect of electric field and phase field on the double bubble deformation and dynamic behavior in static liquid was studied. The following conclusions were obtained:

(i) Comparison of the results with results of the previous researchers in the case of no-electric field effects shows a good agreement.

(ii) For bubble-bubble rising in a fluid, the presence of a vertical electric field increases the rising velocity of the bubbles.

(iii) Applying a uniform electric field causes the bubbles to extend toward the electric field, reducing the minimum distance between the bubbles. Compared with the case of no electric field, the existence of the vertical electric field reduces the coalescence time of the bubble pair.

(iv) When the electric field strength is strong ($E \geq$ 1 kV/mm), the bubble will be broken after coalescence of the bubble.

References

[1] Zhang A M and Yao X L 2008 *Chin. Phys. B* **17** 927
[2] Clift R, Grace J R and Weber M E 1978 *Bubbles, Drops, and Particles* (New York: Academic Press)
[3] Kirkpatrick R D and Lockett M J 1974 *Chem. Eng. Sci.* **29** 2363
[4] Zhang S J and Wu C J 2011 *J. Hydrodyn* **23** 89
[5] Annal, M V S, Deen N G and Kuipers J A M 2005 *Chem. Eng. Sci.* **60** 2999
[6] Cheng M, Hua J S and Lou J 2010 *Comput. Fluid.* **39** 260
[7] Li S B, Xu S, Fan J G and Huang S Y 2017 *J. Shenyang. Inst. Aerona Eng.* **34** 63
[8] Lv Y Q 2016 *Numerical Research on Bubble Merging and its Motion in Shear Flow* (MS Thesis) (Hangzhou: China Jiliang University) (in Chinese)
[9] Hadidi A and Jalali-Vahid D 2016 *Theor. Comput. Fluid. Dyn* **30** 165
[10] Hirt C W and Nichols B D 1981 *J. Comput. Phys.* **39** 201
[11] Abbassi W, Besbes S, Elhajem M, Aissia H B and Champagne J Y 2018 *Comput. Fluids* **161** 47
[12] Osher S and Sethian J A 1988 *J. Comput. Phys.* **79** 12
[13] Nagrath S, Jansen K E and Jr R T L 2005 C *Omput. Method. Appl. M* **194** 4565
[14] Jacqmin D 1999 *J. Comput. Phys.* **155** 96
[15] Yang Q Z, Li B Q, Shao J Y and Ding Y C 2014 *Int. J. Heat Mass. Tran.* **78** 820
[16] Zhang Q Y, Sun D K, Zhang Y F and Zhu M F 2016 *Chin. Phys. B* **25** 066401
[17] Chen S and Doolen G D 1998 *Ann. Rev. Fluid. Mech.* **30** 329
[18] Yue P T, Zhou C F, Jams J, Feng J J and Ollivier-Gooch C F 2006 *J. Comput. Phys.* **219** 47
[19] Wang L L, Li G J, Tian H and Ye Y H 2011 *J. Xi'an JiaoTong Univ.* **45** 65
[20] Ding H, Spelt P D M and Shu C 2007 *J. Comput. Phys.* **226** 2078
[21] Liang M, Li Q, Wang K S, Liu J Y and Chen J Q 2014 *Ciesc. J.* **65** 843
[22] Allen P H G and Karayiannis T G 1995 *Heat Recov. Syst. Chp.* **15** 389